

Communications to the Editor

Fast Long-Range Adiabatic Electron Transfer in a Model Polyglycine α -Helix

Thomas Herz, Peter Gedeck, and Timothy Clark*

Computer-Chemie-Centrum
Friedrich-Alexander-Universität Erlangen-Nürnberg
Nägelsbachstrasse 25, D-91052 Erlangen, Germany

Received October 19, 1998

Long-range electron transfer (ET) in proteins is an important life process¹ that is, however, still only sketchily understood.² Most attempts to understand protein ET concentrate on the calculation or estimation of the electronic matrix coupling element that largely determines the rate of coherent (tunneling) ET over the entire distance that the electron must travel.³ An interesting alternative mechanism that has received little attention is hopping conductivity, proposed by Ladik et al., from ab initio calculations on pig insulin.⁴ We now report semiempirical (AM1⁵) configuration interaction (CI) calculations designed to elucidate the mechanism of long-range ET in model polyglycine α -helices.

In our initial investigations, (Gly)₃₀ in the α -helix conformation was fully optimized with AM1. The optimized geometry was used for single point configuration interaction (CI) calculations including only single excitations (CIS) with an active orbital window of 90 MOs. These were the 30 highest doubly occupied orbitals, the lowest 30 non-doubly occupied orbitals, over which the half-electron approximation⁶ was used to distribute the single electron evenly in the reference wave function, and the lowest 30 unoccupied MOs. This technique corresponds roughly to an improved virtual orbital CI. Analysis of the ground and excited states reveals that the former is a ketyl radical anion localized at Gly₂ and that the latter can usually be described as local ketyl anions situated in different glycine residues. The energies of the lowest 50 states obtained are plotted in Figure 1 against the calculated shift of the charge center relative to the ground state (defined in the figure caption). A series of "local ground state" ketyl radical anions can be seen (black lines) with energies that increase more or less monotonically toward the C-terminus. A corresponding series of "local excited states" (gray lines) show a similar energetic trend and some delocalized states (asterisks) are also observed at higher energies. The energetic cascade of the "local ground states" is caused by interaction of the localized negative charges with the cumulative helix dipole and can be reproduced by a simple point charge/dipole electrostatic model.⁷

(1) Nocek, J. M.; Zhou, J. S.; De Forest, S.; Priyadarshy, S.; Beratan, D. N.; Onuchic, J. N.; Hoffman, B. M. *Chem. Rev.* **1996**, *96* (No. 7), 2459. Deisenhofer, J.; Norris, J. R. *The Photosynthetic Reaction Center*; Academic Press: San Diego, 1993; Vol. I.

(2) Jortner, J.; Ratner, M. In *Molecular Electronics: a "chemistry for the 21st century monograph"*; Jortner, J., Ratner, M., Ed.; IUPAC/Blackwell: Oxford, 1997; Chapter 1.

(3) Kuki, A. Long-range electron transfer in biology. In *Structure and bonding*, 75; Palmer, G. A., Ed.; Springer: New York, 1991. Therien, M. J.; Chang, J.; Raphael, A. L.; Bowler, B. E.; Gray, H. B. Long-range electron transfer in biology. In *Structure and bonding*, 75; Palmer, G. A., Ed.; Springer: New York, 1991.

(4) Ye, Y.-J.; Ladik, J. *Phys. Rev.* **1993**, *B 48*, 5120.

(5) Dewar, M. J. S.; Zoebisch, E. G.; Healy, E. F.; Stewart, J. J. P. *J. Am. Chem. Soc.* **1985**, *107*, 3902.

(6) Dewar, M. J. S.; Hashmall, J. A.; Venier, C. G. *J. Am. Chem. Soc.* **1968**, *90*, 1953.

(7) Rauhut, G.; Clark, T. *J. Comput. Chem.* **1993**, *14*, 503. Beck, B.; Rauhut, G.; Clark, T. *J. Comput. Chem.* **1994**, *15*, 1064.

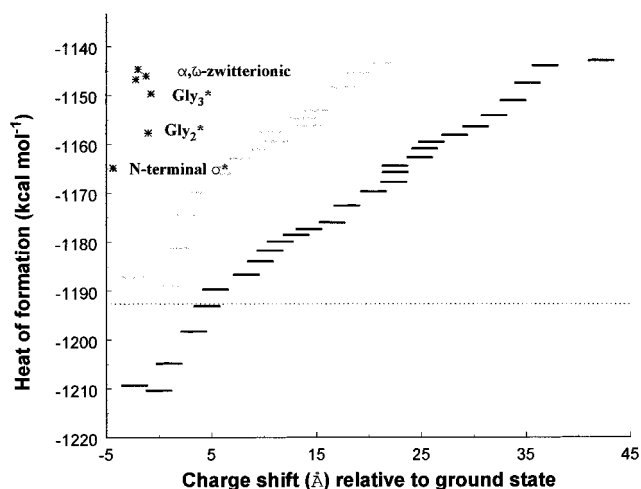


Figure 1. Plot of the AM1-calculated heats of formation¹¹ of the lowest 50 states of (Gly)₃₀^{•-} at the geometry of the neutral helix against the calculated shift of the center of charge from that of the ground state. Positive distances indicate a shift toward the C-terminus. The charge shift vector $\Delta\mathbf{r}$ is defined as the distance between the center of charge of the reference (ground) state and that of the state being considered. Within the NAO-PC approximation⁷ it is calculated as $\Delta\mathbf{r} = \sum_1^N [\mathbf{r}_N q_N - \mathbf{r}_N^0 q_N^0] / \sum_1^N q_N$, where N is the total number of NAO-PCs, \mathbf{r} and \mathbf{r}^0 are the vector distances from the origin to the NAO-PC in the state being considered and the reference state, respectively, and q and q^0 are the corresponding charges. The meanings of the different symbols used are explained in the text. The horizontal dotted line indicates the heat of formation of the neutral α -helix.

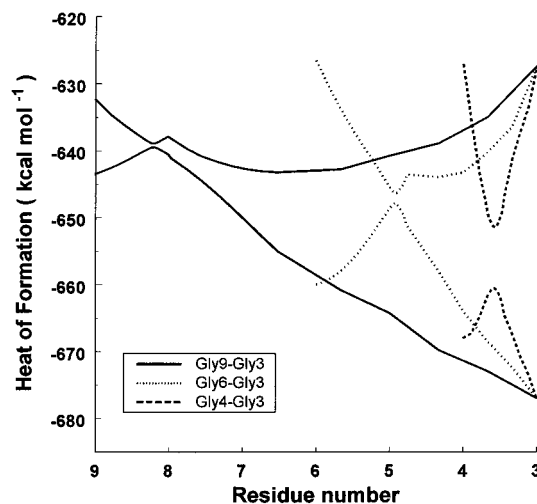


Figure 2. Calculated linear synchronous transit energy profiles for the ground and first excited states for 1,7-, 1,4-, and 1,2-ET in (Gly)₁₇^{•-}. The horizontal axis is labeled according to residue number, although these strictly only apply to the end points of the three reaction profiles.

The above results suggest that the hopping conductivity mechanism suggested by Ladik et al.⁴ may be operative. This would be an attractive result because it would suggest that α -helices are essentially ohmic conductors with an approximately r^{-1} rate dependence on the ET distance r .² To test this hypothesis, we needed to investigate different possible ET reactions. Because the helix structure is strongly distorted when the geometries of

Table 1. Calculated Rates (s^{-1}) for Unimolecular Electron Transfers between Localized Ketyl Anion States in a $(\text{Gly})_{17}^{\bullet-}$ α -Helix Radical Anion

	1,2-ET		1,4-ET		1,7-ET	
	Gly ₄ -Gly ₃	Gly ₃ -Gly ₂	Gly ₆ -Gly ₃	Gly ₅ -Gly ₂	Gly ₉ -Gly ₃	Gly ₈ -Gly ₂
adiabatic ⁹	8.8×10^7	3.1×10^7	3.6×10^4	5.8×10^4	2.9×10^{10}	3.4×10^9
nonadiabatic ¹⁰	8.1×10^5	9.6×10^4	4.6×10^3	6.4×10^3	1.4×10^9	2.4×10^8

the local anion states are optimized, we applied weak harmonic positional constraints to the α -carbons of the helix backbone⁸ to optimize the geometries of local ketyl states in a model $(\text{Gly})_{17}^{\bullet-}$ α -helix with UHF/AM1 while retaining the helix structure (this procedure mimics the effect of the surrounding protein in an enzyme). These geometries were used for linear synchronous transit AM1/CIS calculations with 35 active orbitals to investigate the energy profiles for different ET processes. The results are shown in Figure 2.

Surprisingly, the 1,7-ET from Gly₉ to Gly₃ shows a lower activation energy ($4.0 \text{ kcal mol}^{-1}$) than the 1,4-process from Gly₆ to Gly₃ ($12.1 \text{ kcal mol}^{-1}$), whereas the 1,2-ET from Gly₄ to Gly₃ is intermediate ($7.5 \text{ kcal mol}^{-1}$). These results suggest that there is no need to invoke the hopping mechanism. The 1,7-ET calculations do not support the hypothesis that electronic coupling through the $\text{NH}\cdots\text{O}=\text{C}$ hydrogen bond is a major factor in determining protein ET rates. The splitting between the ground and first excited states at the highest points on the reaction profiles is 9.2, 1.5, and $0.6 \text{ kcal mol}^{-1}$ for the 1,2-, 1,4-, and 1,7-ET processes, revealing either a very weak or no extra coupling due to the hydrogen bonds in the 1,4- and 1,7-cases. We have calculated ET rates for the three processes using both the adiabatic⁹ and the nonadiabatic¹⁰ rate models. The results are shown in Table 1. Our results show that the calculated adiabatic

(8) Gedeck, P.; Schürer, G.; Clark, T. manuscript in preparation. The α -carbons were constrained to their optimized positions in the neutral helix with a force constant of $10 \text{ kcal mol}^{-1} \text{ \AA}^{-1}$.

(9) An inner vibrational frequency $\nu_1 = 1600 \text{ cm}^{-1}$, corresponding to the C=O stretching frequency, was used for the adiabatic rate calculations, which used the expression $k_{\text{ET}} = (\nu_1/2)e^{-\Delta G^\ddagger/k_{\text{B}}T}$ defined in: Sutin, N. *Prog. Inorg. Chem.* **1983**, *30*, 441.

rate constants are consistently higher than the nonadiabatic ones. Most importantly, however, they suggest very fast ET over distances of 10 \AA or more toward the N-terminus of α -helices. The calculated rates are considerably faster than those observed experimentally,³ but we emphasize that they refer to real ET within the helix, not the virtual ET process usually observed.

The current calculations¹¹ apply to a model system in vacuo without charged side chains and will be modified by the effect of the dielectric protein environment, which we are now including in our model systems. However, the high calculated rates obtained suggest that a similar treatment for more realistic systems will still reproduce experimentally observed fast long-range ET rates.

Acknowledgment. Dedicated to Keith Ingold on the occasion of his 70th birthday. This work was supported by the Volkswagen Foundation, the Deutsche Forschungsgemeinschaft as part of the Graduiertenkolleg "Homogene und Heterogene Elektronentransfer" and the Fonds der Chemischen Industrie.

JA9836500

(10) The adiabatic rate constants were calculated with use of the expression

$$k_{\text{ET}} = \frac{2V_{12}^2}{h} \sqrt{\left(\frac{\pi^3}{\lambda k_{\text{B}}T}\right)} e^{-\Delta G^\ddagger/k_{\text{B}}T}$$

defined in: Hush, N. S. *Coord. Chem. Rev.* **1985**, *64*, 135. A value for the reorganization energy $\lambda = 50 \text{ kcal mol}^{-1}$ was determined from the calculated potential energy curves.

(11) All calculations were performed with VAMP 7.0 (Gedeck, P.; Burkhardt, F.; Horn, A.; Beck, B.; Rauhut, G.; Alex, A.; Chandrasekhar, J.; Steinke, T.; Sauer, W.; Hutter M.; Clark, T. *Vamp 7.0*, Oxford Molecular, The Medawar Centre, Oxford Science Park, Sandford-on-Thames, Oxford OX4 4GA, United Kingdom, 1998). The techniques used are defined in: Stewart, J. J. P. *J. Comput. Aided Mol. Design* **1990**, *4*, No. 1.